Electronic Supplementary Information

Encapsulation of dihydrogenphosphate ions as a cyclic dimer to the cavities of site-specifically modified indolocarbazole-pyridine foldamers†‡

Chaeeun Lee,§ Hyemi Lee,§ Seungwon Lee, Hae-Geun Jeon and Kyu-Sung Jeong*

**Department of Chemistry, Yonsei University, Seoul, Korea*

Fax: +82-2-364-7050

Tel: +82-2123-2643

E-mail: ksjeong@yonsei.ac.kr

† Dedicated to Prof. Julius Rebek Jr. on occasion of his 75th birthday.

‡ Electronic supplementary information (ESI) available. See DOI:

§ These authors contributed equally to this work.

Contents

1. Syntheses and spectroscopic properties of new compounds

1.1 General: All chemicals were purchased from commercial suppliers and used without further purification unless otherwise specified. Dichloromethane (CH_2Cl_2) was purified by drying over calcium hydride (CaH_2), followed by distillation. Hexane, ethyl acetate (EtOAc), and acetone were distilled. Water-saturated CD_2Cl_2 was prepared by sonication of a mixture of solvent containing a few drops of distilled water for 30 min. After 1 h standing, organic layer was carefully separated out for use. Thin layer chromatography (TLC) was performed on Merck (silica gel 60, F-254, 0.25 mm). Silica gel 60 (230-400 mesh, Merck) was used for column chromatography. Melting points were determined with a Barnstead Electrothermal (IA9100) apparatus. 1D and 2D NMR spectra were measured by using Bruker Avance II DRX 400 and Avance III HD 300 instruments. Chemical shifts were reported using residual protonated solvent peaks (for ^{1}H NMR spectra, acetone-d_6 2.05 ppm; CD_2Cl_2 5.32 ppm; $CDCl_3$ 7.26 ppm; DMSO-d_6 2.50 ppm and for ^{13}C NMR spectra, acetone-d_6 206.26 ppm; CD_2Cl_2 53.84 ppm). FT-IR spectra were measured by using a Vertex70 FT-IR spectrometer. Gas chromatographic analysis was performed on Agilent 7890A instrument with FID detector. MALDI-TOF mass spectrometric measurements were performed on a Bruker (LRF20). The ESI-HRMS spectrometric measurements were obtained from *the Organic Chemistry Research Center* at Sogang University.

1.2 Synthesis of compound **2**

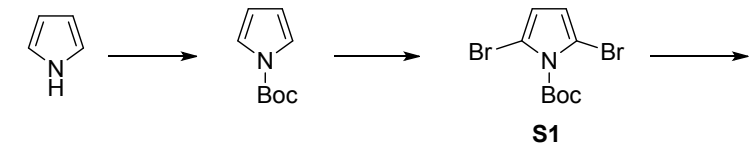

S1

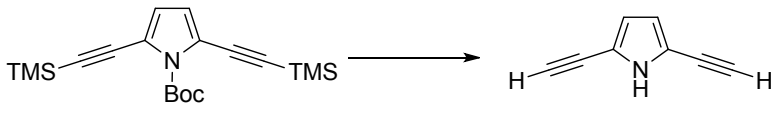

S2 **S3**

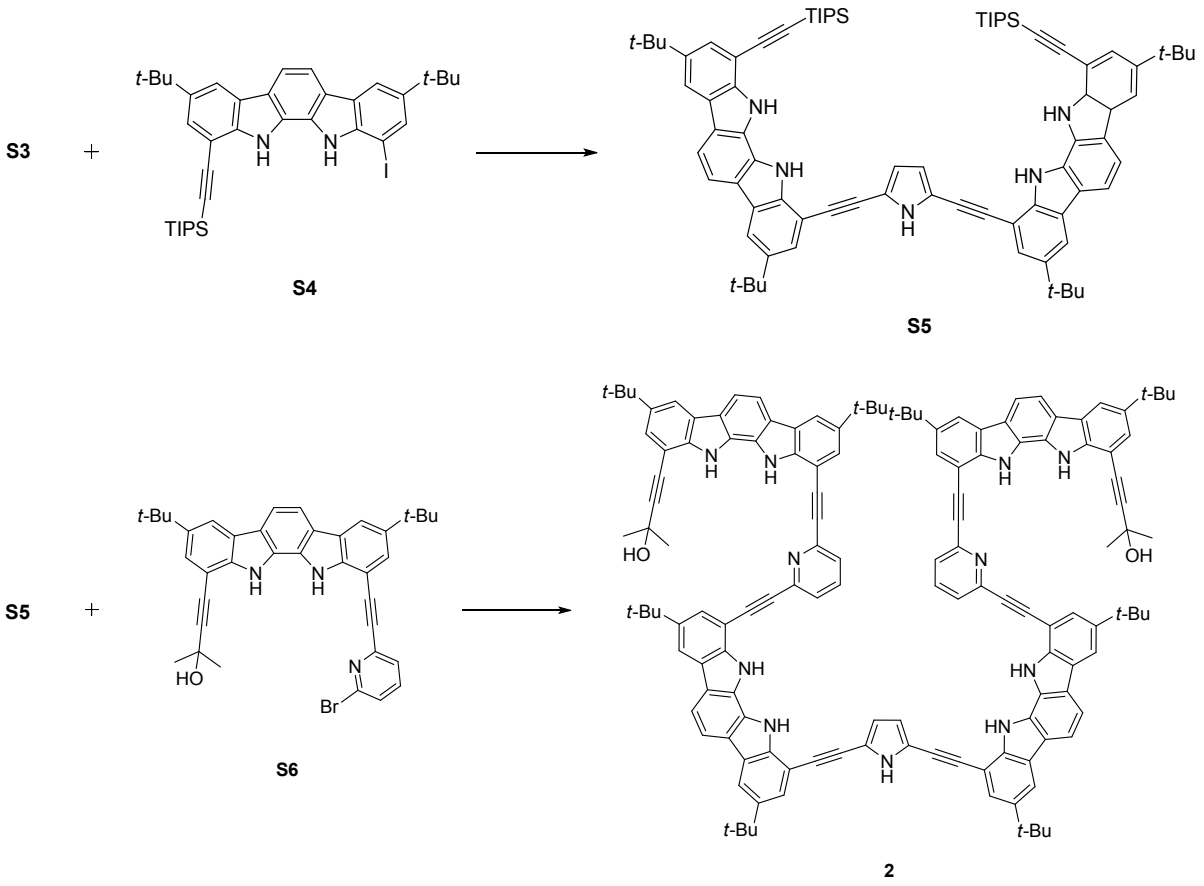

S2: The synthesis of **S1** was prepared following the procedures described in a literature.[S1] A Schlenk flask containing compound **S1** (4.7 g, 14.5 mmol), CuI (84 mg, 0.03 equiv) and $Pd(PPh_3)_2Cl_2$ (308 mg, 0.03 equiv) was evacuated under vacuum and back-filled with nitrogen. Degassed triethylamine (Et_3N) (40 mL), tetrahydrofuran (THF) (35 mL) and trimethylsilyl-acetylene (11 mL, 5.5 equiv) were added in order and the solution was stirred at 55 °C for 10 h. The mixture was filtered through Celite and concentrated, and the residue was dissolved in CH_2Cl_2. The organic solution was washed with brine and saturated $NaHCO_3$ solution, dried over anhydrous Na_2SO_4 and concentrated. The residue was purified by flash column chromatography (silica gel, CH_2Cl_2/hexane = 1:3 (*v*/*v*)) to give **S2** as a reddish brown solid (4.3 g, 82%); mp: 64 °C; ^{1}H NMR (400 MHz, acetone-d_6, 298 K, ppm) δ 6.53 (s, 2H), 1.66 (s, 9H), 0.24 (s, 18H); ^{13}C NMR (100 MHz, acetone-d_6, 298 K, ppm) δ 147.2, 119.6, 116.7, 99.1, 95.9, 85.2, 27.1, -0.94; MALDI-TOF *m/z* calcd for $C_{19}H_{29}NO_2Si_2$ 359, found 358; IR (thin film) υ 2151 (C≡C), 1761 (C=O), 1171 (C-O) cm^{-1}.

[S1] F. Ferenc, D. Szilvia, M. Zoltan, H. Tamas, B. Laszlo, S. Boros, B. Barbara, H. Tamas, N. Miklos and M. Bela, *Tetrahedron*, 2016, **72**, 5444-5455.

^{1}H NMR spectrum of **S2** in acetone-d_6

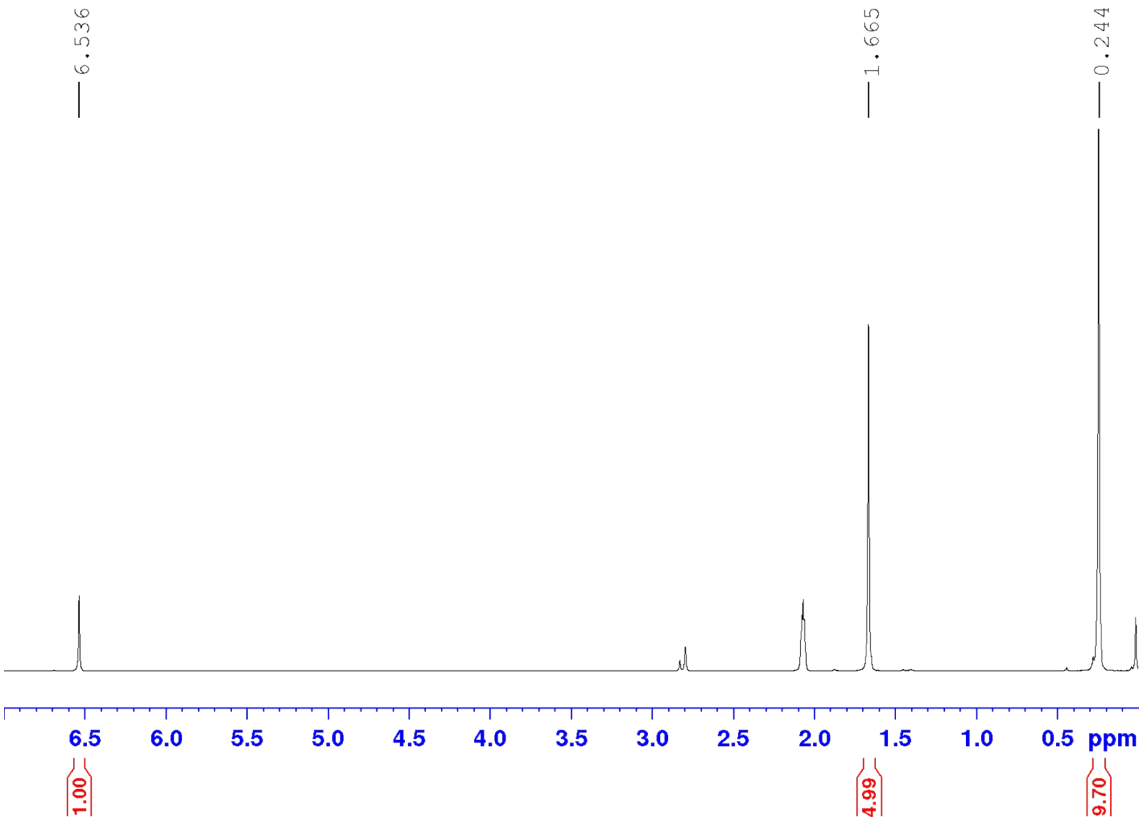

^{13}C NMR spectrum of **S2** in acetone-d_6

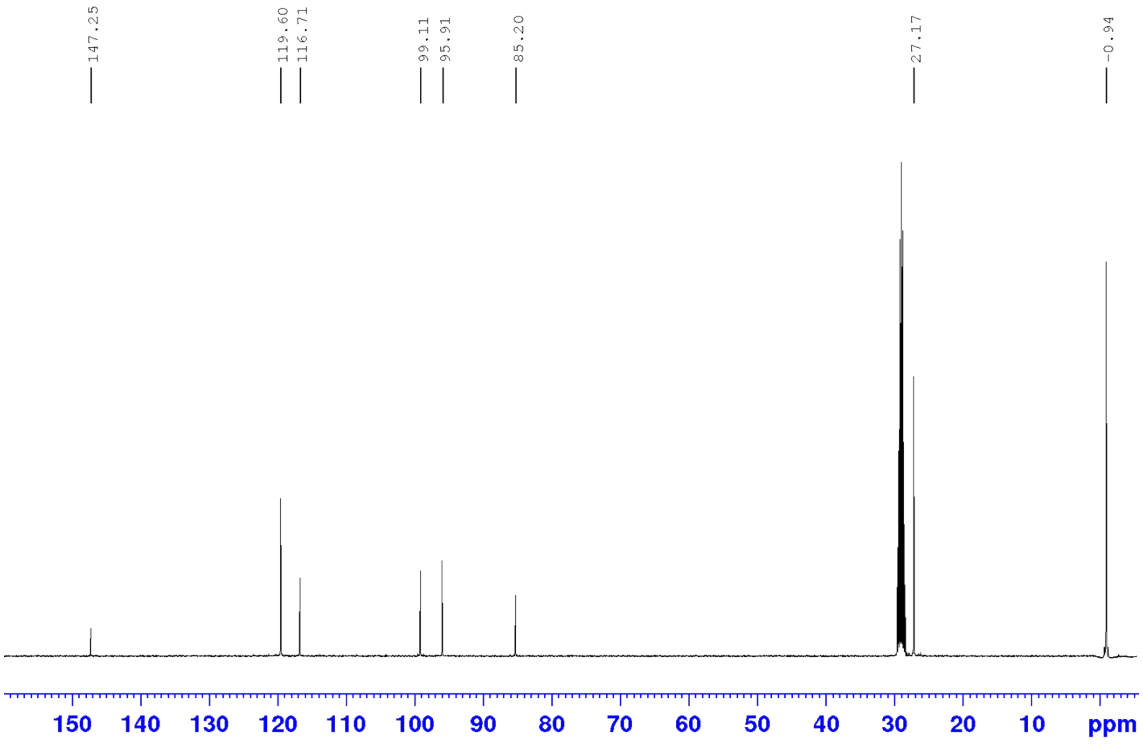

S3: Compound **S2** (125 mg, 0.35 mmol, 1 equiv) was added to a 50 mL round bottom flask and dissolved in THF (2 mL) and MeOH (2 mL). K_2CO_3 (242 mg, 1.75 mmol, 5 equiv) was sequentially added and the solution was stirred at room temperature for 2 h. The reaction mixture was filtered through Celite using CH_2Cl_2, and washed with brine and then dried over anhydrous Na_2SO_4. The crude product was purified by flash column chromatography (silica gel, CH_2Cl_2 : hexane = 1 : 1 (*v*/*v*)) to give **S3** (28 mg, 70%); ^{1}H NMR (400 MHz, acetone-d_6, 298 K, ppm) δ 11.07 (s, 1H, NH), 6.39 (s, 2H), 3.69 (s, 2H); ^{13}C NMR (100 MHz, acetone-d_6, 298 K, ppm) δ 115.9, 114.0, 80.2, 80.2, 76.4; GC/MS m/*z* calcd for C_8H_5N $[M]^+$ 115, found 115; IR (thin film) υ 3293(NH), 2107 (C≡C) cm $^{-1}$.

^{1}H NMR spectrum of **S3** in acetone-d_6

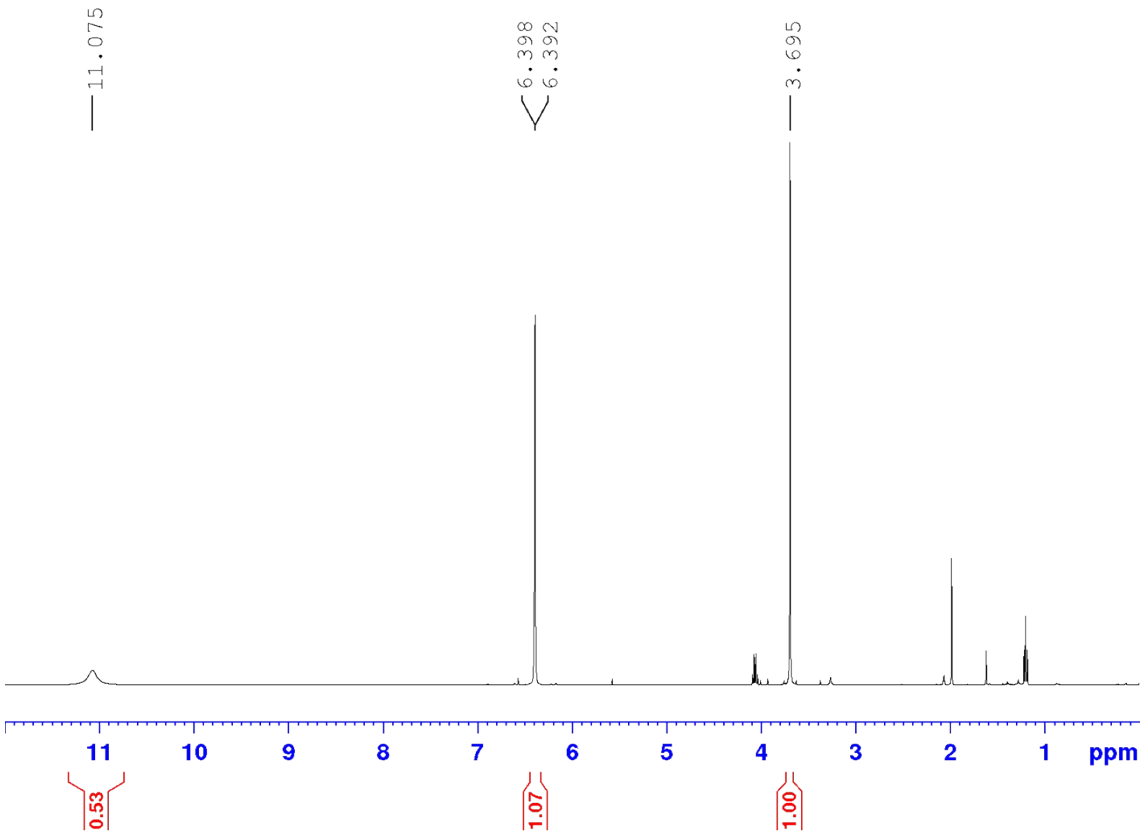

^{13}C NMR spectrum of **S3** in acetone-d_6

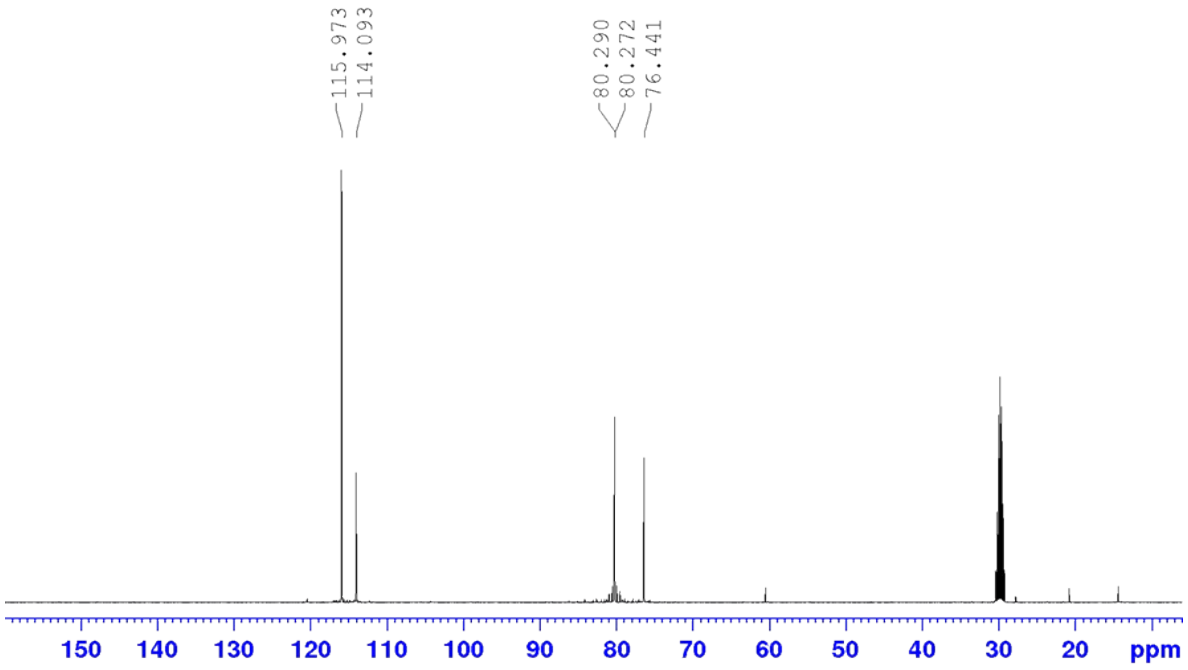

S5: The synthesis of **S4** was described previously.[S2] A Schlenk flask containing compound **S3** (1.15 g, 1.7 mmol, 2 equiv), **S4** (98 mg, 0.85 mmol, 1 equiv), CuI (5 mg, 0.03 equiv) and $Pd(PPh_3)_2Cl_2$ (18 mg, 0.03 equiv) was evacuated under vacuum and back-filled with nitrogen. Degassed Et_3N (9 mL) and THF (8 mL) were added in order and the solution was stirred at room temperature overnight. The mixture was filtered through Celite and concentrated, and the residue was dissolved in CH_2Cl_2. The organic solution was washed with brine and saturated $NaHCO_3$ solution, dried over anhydrous Na_2SO_4 and concentrated. The residue was purified by flash column chromatography (silica gel, CH_2Cl_2/hexane = 1:5 (*v*/*v*)) to give **S5** as a green solid (480 mg, 48%); mp > 264 °C (dec); ^{1}H NMR (400 MHz, acetone-d_6, 298 K, ppm) δ 11.42 (s, 1H, NH), 10.29 (s, 2H, NH), 10.23 (s, 2H, NH), 8.33 (s, 4H), 8.05 (s, 4H), 7.65 (t, J = 1.8 Hz, 4H), 6.71 (s, 2H), 1.50 (s, 9H, *t*-Bu), 1.46 (s, 9H, *t*-Bu), 1.15 (s, 18H, *t*-Bu); ^{13}C NMR (100 MHz, acetone-d_6, 298 K, ppm) δ 143.4, 143.3, 139.2, 138.9, 138.8, 127.7, 127.7, 126.9, 126.8, 126.8, 125.9, 125.9, 125.4, 125.1, 122.6, 122.5, 118.5, 118.4, 118.2, 116.1, 115.7, 115.6, 113.3, 113.2, 106.2, 105.8, 105.2, 94.7, 88.4, 86.3, 35.3, 35.2, 32.2, 32.1, 19.0, 12.1; MALDI-TOF *m/z* calcd for $C_{82}H_{99}N_5Si_2$ 1209, found 1208; IR (thin film) υ 3355(NH), 2207 (C≡C) cm^{-1}.

[S2] J. S. Kim, H.-G. Jeon and K.-S. Jeong, *Chem. Commun.*, 2016, **52**, 3406–3409.

^{1}H NMR spectrum of **S5** in acetone-d_6

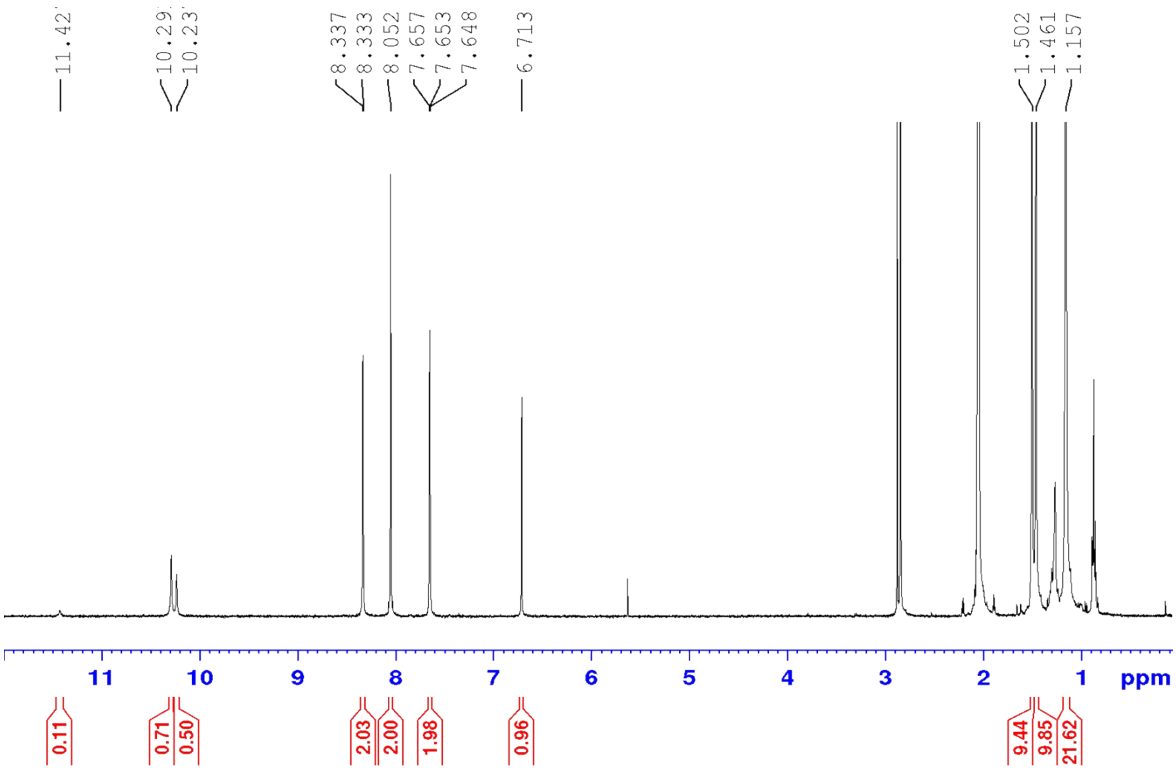

^{13}C NMR spectrum of **S5** in acetone-d_6

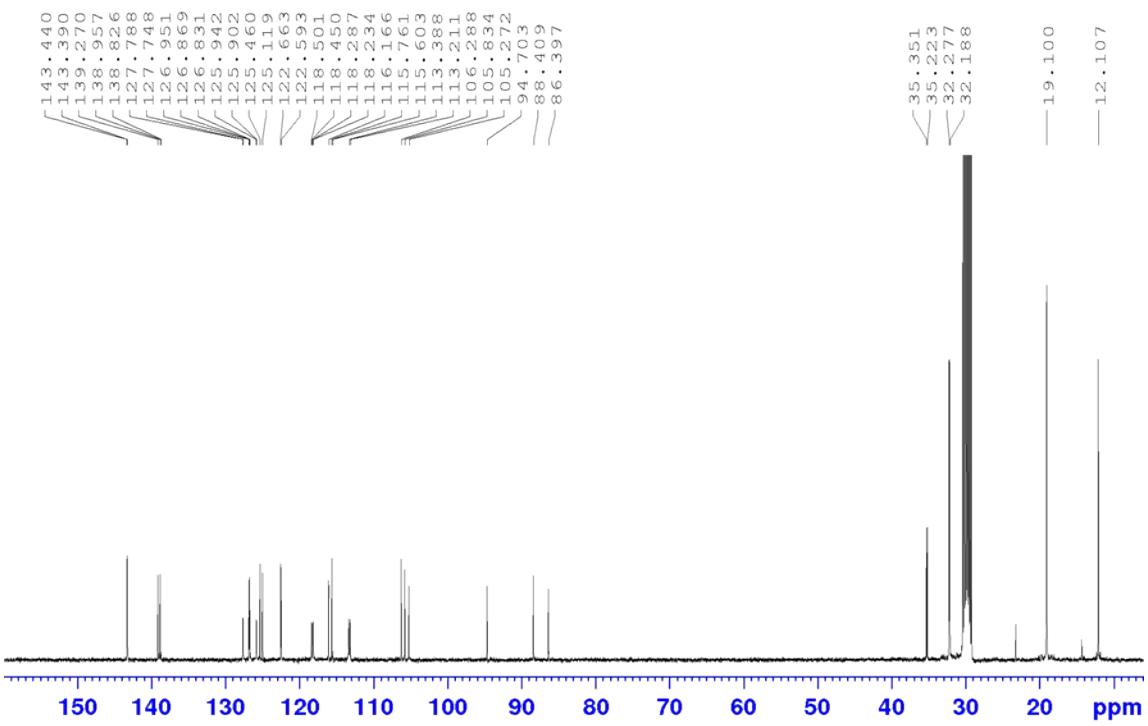

2: The synthesis of **S6** was described previously.[S2] A Schlenk flask containing compound **S6** (158 mg, 0.24 mmol, 2 equiv), **S5** (150 mg, 0.12 mmol, 1 equiv), CuI (5 mg, 0.2 equiv) and $Pd(PPh_3)_2Cl_2$ (18 mg, 0.2 equiv) was evacuated under vacuum and back-filled with nitrogen. Degassed THF (2 mL) and tetrabutylammonium fluoride (TBAF) (0.4 mL, 3 equiv) were added in order and the solution was stirred at room temperature for 10 min. After adding Et_3N (2.1 mL), the solution was stirred at 50 °C for 14 h. The mixture was filtered through Celite and concentrated, and the residue was dissolved in CH_2Cl_2. The organic solution was washed with brine and saturated $NaHCO_3$ solution, dried over anhydrous Na_2SO_4 and concentrated. The residue was purified by flash column chromatography (silica gel, hexane/ EtOAc = 1:1 (*v*/*v*)) to give **2** as an orange solid (150 mg, 60%); mp > 257 °C (dec); ^{1}H NMR (400 MHz, CD_2Cl_2, 298 K, ppm) δ 11.15 (s, 1H, NH), 10.37 (s, 2H, NH), 9.40 (s, 2H, NH), 9.26 (s, 2H, NH), 9.11 (s, 2H, NH), 8.39 (s, 2H), 7.98 (s, 2H), 7.96 (s, 2H), 7.88 (s, 2H), 7.84 (s, 2H), 7.79 (d, J = 8.45 Hz, 2H), 7.77 (d, J = 8.56 Hz, 2H), 7.69 (d, J = 8.22Hz, 2H), 7.32 (s, 2H), 7.20 (s, 2H), 7.10 (s, 2H), 7.10 (s, 2H), 6.48 (t, J = 7.70 Hz, 2H), 6.13 (d, J = 7.81 Hz, 2H), 6.01 (d, J = 7.56 Hz, 2H), 1.59 (s, 9H, *t*-Bu), 1.50 (s, 9H, *t*-Bu), 1.45 (s, 9H, *t*-Bu), 1.43 (s, 9H, *t*-Bu), 1.30 (s, 6H); ^{13}C NMR (100 MHz, acetone-d_6, 298 K, ppm) δ 143.7, 143.7, 142.7, 142.6, 142.5, 142.3, 138.5, 138.3, 138.3, 138.0, 137.0, 126.7, 126.2, 126.1, 126.0, 125.9, 125.8, 125.7, 125.4, 124.6, 124.2, 124.1, 121.8, 121.7, 121.5, 121.4, 118.4, 117.4, 116.7, 115.3, 114.6, 112.5, 112.4, 112.3, 105.3, 104.9, 103.8, 103.7, 99.0, 92.1, 92.0, 87.3, 86.5, 85.3, 77.5, 64.5, 34.5, 34.4, 34.4, 34.3, 31.4, 31.2; MALDI-TOF *m/z* calcd for $C_{140}H_{127}N_{11}O_2$ $[M]^+$ 1994, found 1993; ESI-HRMS *m/z* calcd for $C_{140}H_{128}N_{11}O_2$ $[M+H]^+$ 1996.0286, found 1996.0289; IR (thin film) υ 3530 (OH) , 3346(NH), 2205 (C≡C), 1161 (C-O) cm^{-1}.

^{1}H NMR spectrum of **2** in CD_2Cl_2

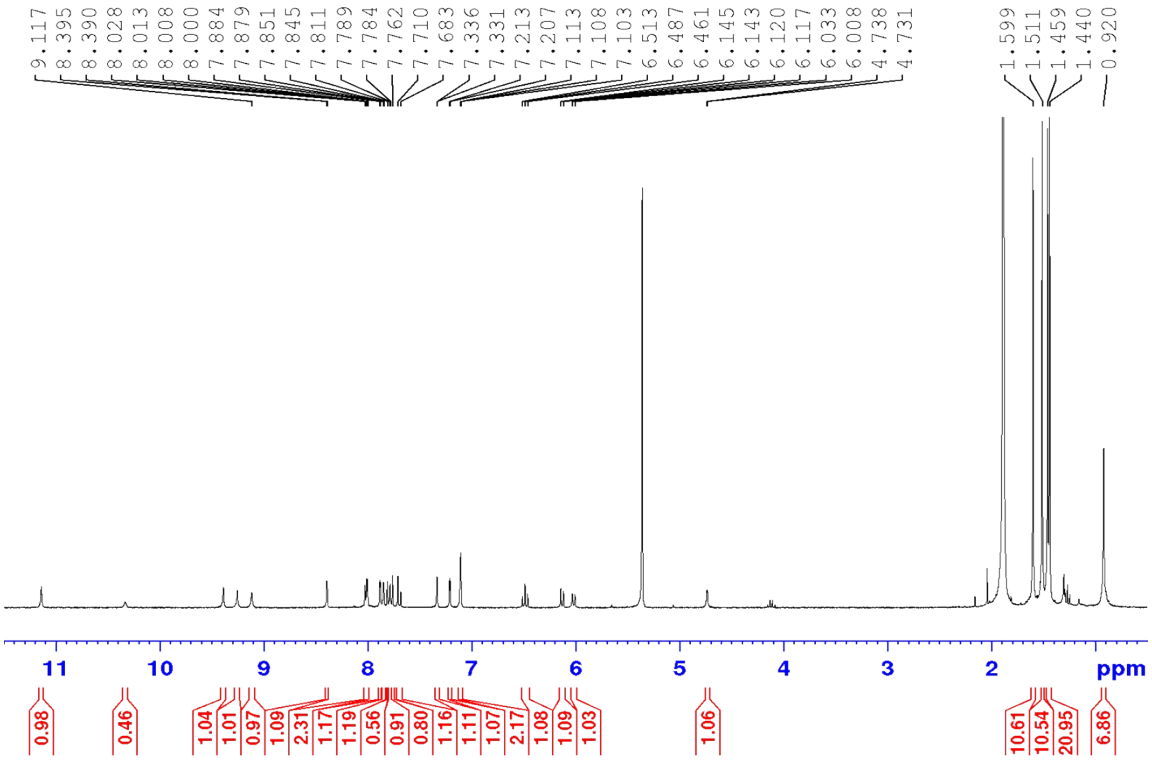

^{13}C NMR spectrum of **2** in acetone-d_6

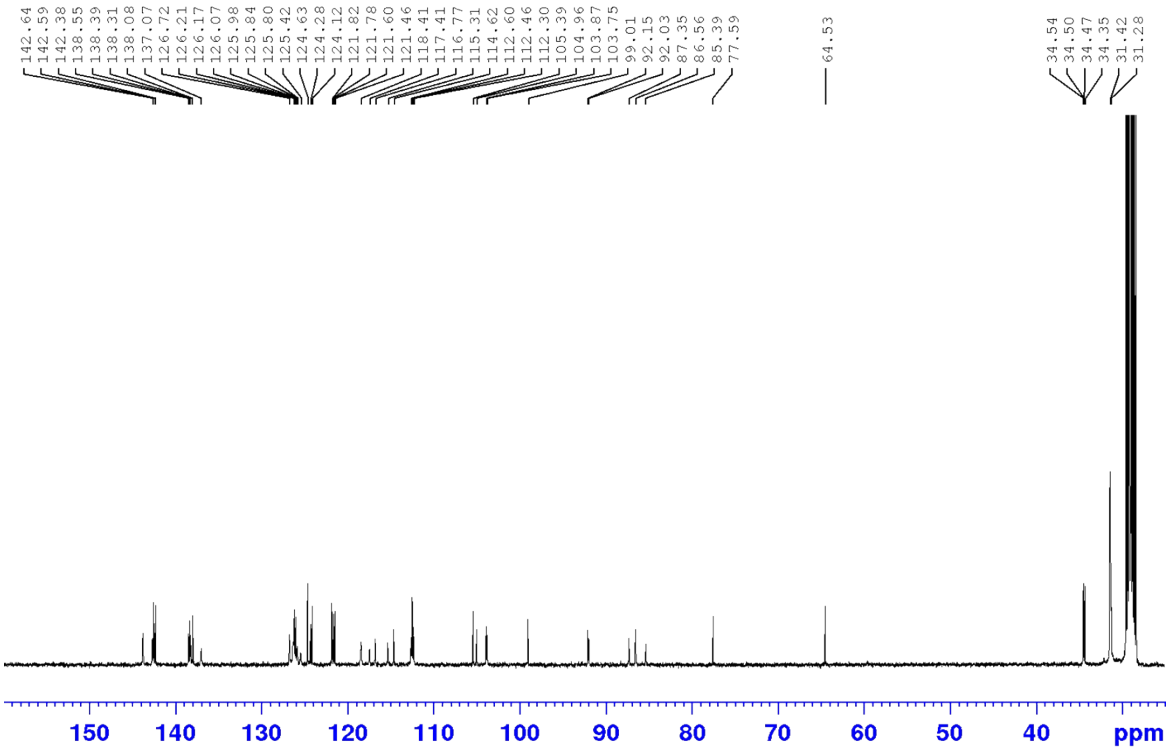

1.3 Synthesis of compound **3**

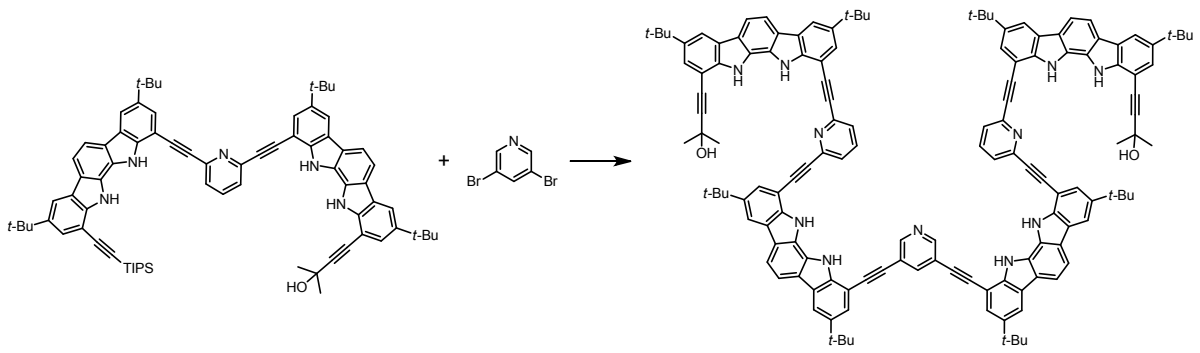

S7 **3**

3: The synthesis of **S7** was described previously.[S2] Schlenk flask containing **S7** (0.38 g, 0.338 mmol), 3,5-dibromopyridine (0.038 g, 1 equiv), CuI (3.2 mg, 0.05 equiv), $Pd(PPh_3)_2Cl_2$ (12 mg, 0.05 equiv) was evacuated under vacuum and back-filled nitrogen. Anhydrous, degassed THF (3.0 mL), Et_3N (4.0 mL) and TBAF (0.5 mL, 1.5 equiv) were added in order to the solution and the mixture was stirred at 55 °C for 4 h. The residue was filtered through Celite and the residue dissolved in CH_2Cl_2. The mixture washed with brine, dried over anhydrous Na_2SO_4. After concentrated, the residue was purified by flash column chromatography (silica gel, diethyl ether) to give compound **3** as a yellow solid (205 mg, 63%); mp > 251 °C (dec); ^{1}H NMR (400 MHz, CD_2Cl_2, 298 K, ppm) δ 11.48 (s, 2H; NH), 9.58 (s, 2H; NH), 9.30 (s, 2H; NH), 9.21 (s, 2H; NH), 8.35 (s, 2H), 8.03 (s, 2H), 8.01 (d, J = 8.3 Hz, 2H), 7.92 (s, 2H), 7.88 (d, J = 8.1 Hz, 2H), 7.77 (d, J = 8.1 Hz, 2H), 7.76 (s, 2H), 7.63 (d, J = 8.2 Hz, 2H), 6.54 (s, 2H), 7.35 (s, 2H), 7.14 (s, 2H), 6.99 (s, 2H), 6.98 (s, 2H), 6.58 (s, 2H), 6.53 (t, J = 7.8 Hz, 2H), 6.03 (d, J = 7.7 Hz, 2H), 6.00 (d, J = 7.7 Hz, 2H), 1.59 (s, 18H, *t*-Bu), 1.45 (s, 18H, *t*-Bu), 1.39 (s, 18H, *t*-Bu), 1.39 (s, 18H, *t*-Bu), 0.80 (s, 12H, Me), 0.66 (s, 2H; OH); ^{13}C NMR (100 MHz, acetone-d_6, 298 K, ppm) δ 151.2, 144.2, 144.2, 143.5, 143.4, 143.2, 143.1, 139.6, 139.3, 139.2, 138.9, 137.3, 127.1, 126.9, 126.8, 126.6, 125.3, 125.0, 122.6, 122.5, 122.3, 120.7, 119.1, 118.9, 117.5, 113.3, 106.2, 105.1, 104.9, 104.6, 99.7, 93.1, 92.8, 91.2, 90.0, 87.4, 78.4, 65.4, 35.4, 35.3, 35.2, 32.3, 32.3, 32.1; MALDI-TOF *m/z* calcd for $C_{141}H_{127}N_{11}O_2$ 2006, found 2007; ESI-HRMS *m/z* calcd for $C_{141}H_{127}N_{11}O_2$ $[M+H]^+$ 2008.0286, found 2008.0266; IR (thin film) υ 2207 (C≡C), 1160 (C-O) cm $^{-1}$.

^{1}H NMR spectrum of **3** in CD_2Cl_2

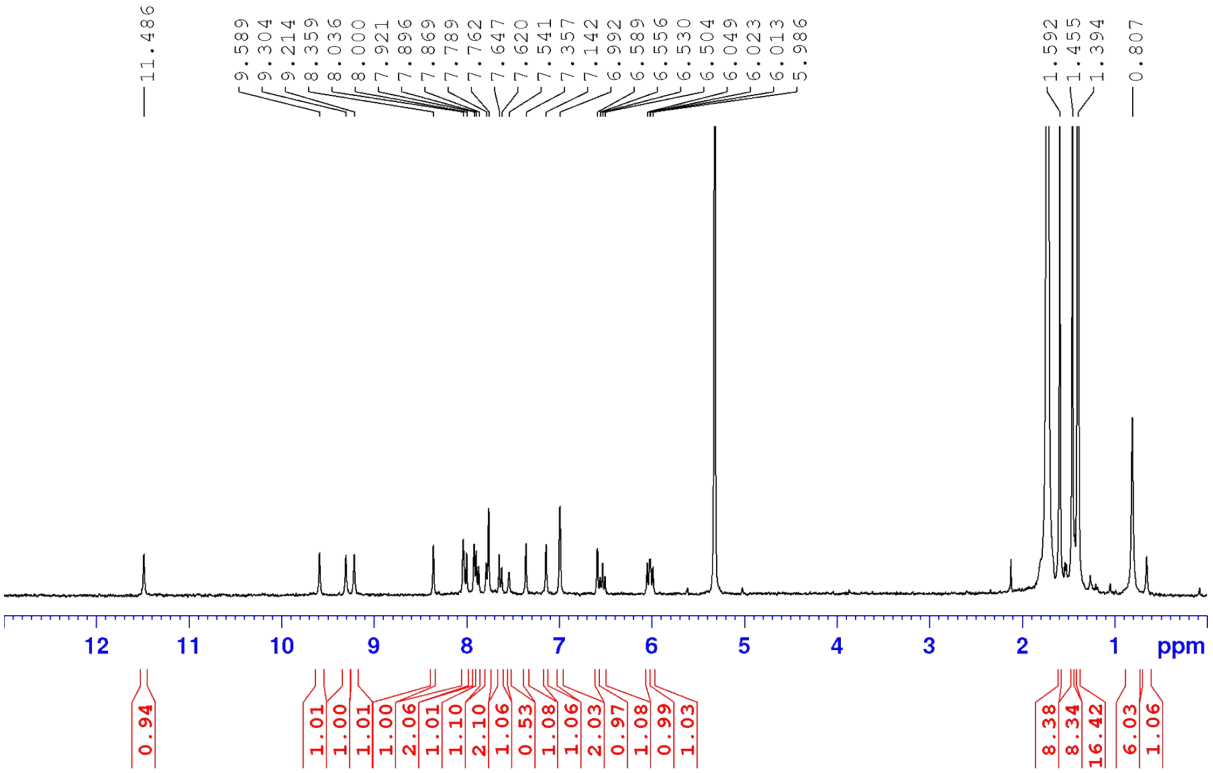

^{13}C NMR spectrum of **3** in acetone-d_6

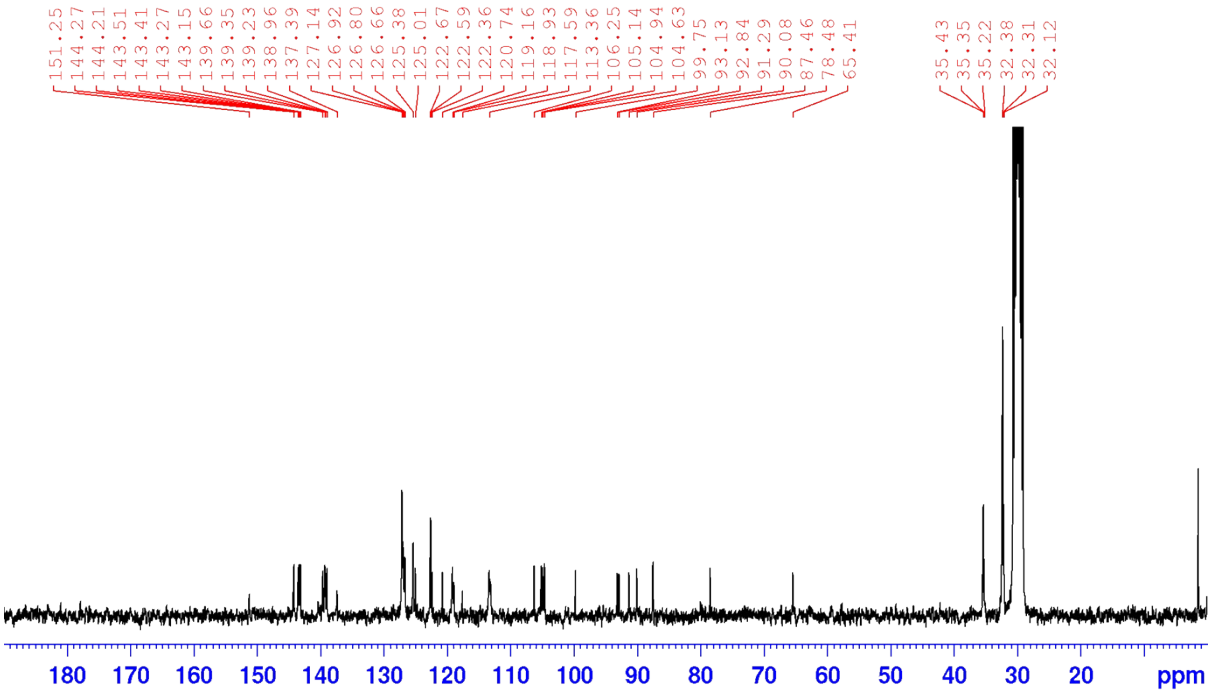

2. ^{1}H NMR studies

2.1 ^{1}H NMR spectra of **2** and **3** in DMSO-d_6 and water-saturated CD_2Cl_2

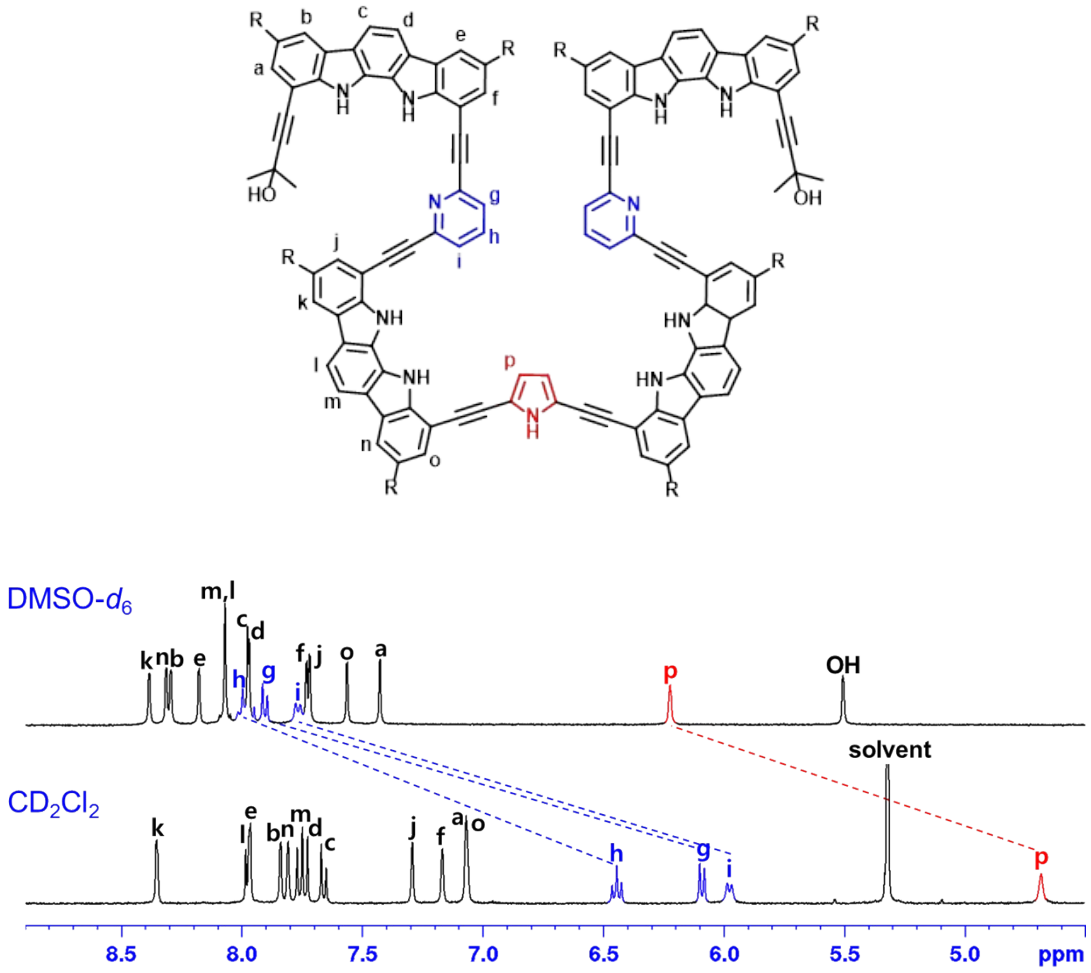

Fig. S1 Partial ^{1}H NMR spectra (25 °C) of **2** (2.0 mM) in DMSO-d_6 and water-saturated CD_2Cl_2. The red- and blue-coloured peaks correspond to the CH signals of central pyrrole and two outer pyridines, respectively.

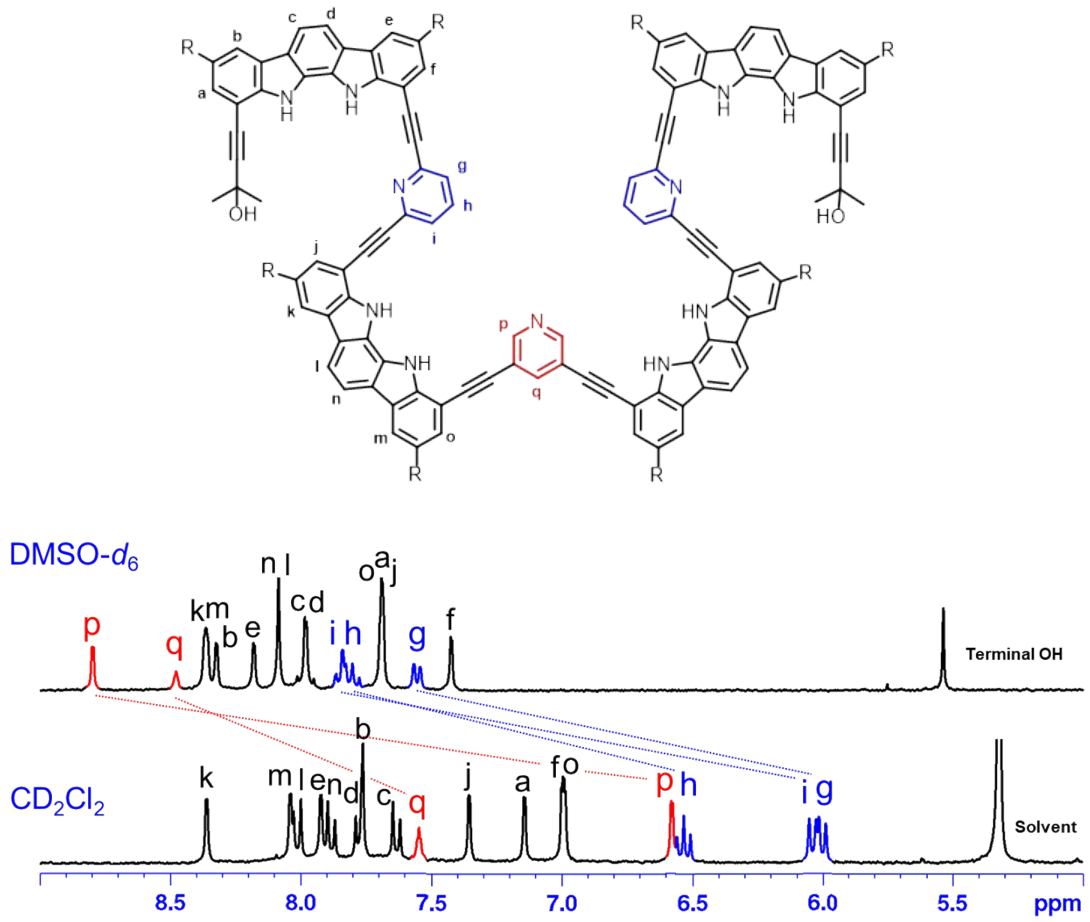

Fig. S2 Partial ^{1}H NMR spectra (25 °C) of **3** (2.0 mM) in DMSO-d_6 and water-saturated CD_2Cl_2. The red- and blue-coloured peaks correspond to the CH signals of central pyridine and two outer pyridines, respectively.

Table. S1 ^{1}H NMR chemical shifts (ppm) and their differences of **2** and **3** (2.0 mM) in water-saturated CD_2Cl_2 and DMSO-d_6 at 298 K.

		δ in CD_2Cl_2	δ in DMSO-d_6	δ (DMSO-d_6) – δ (CD_2Cl_2)
2	a	7.10 (s)	7.43 (s)	0.33
	b	7.88 (s)	8.30 (s)	0.42
	c	7.69 (d, J = 8.22 Hz)	7.98 (d, J = 8.44 Hz)	0.29
	d	7.77 (d, J = 8.56 Hz)	7.97 (d, J = 8.54 Hz)	0.2
	e	7.96 (s)	8.18 (s)	0.22
	f	7.20 (s)	7.73 (s)	0.53
	g	6.13 (d, J = 7.81 Hz)	7.90 (d, J = 7.73Hz)	1.77
	h	6.48 (t, J = 7.70 Hz)	8.01-7.94 (m)	1.49
	i	6.01 (d, J = 7.56 Hz)	7.76 (d, J = 7.73 Hz)	1.75

	j	7.32 (s)	7.72 (s)	0.4
	k	8.39 (s)	8.40 (s)	0.01
	l	7.98 (s)	8.08 (s)	0.1
	m	7.79 (d, *J* = 8.45 Hz)	8.08 (s)	0.29
	n	7.84 (s)	8.32 (s)	0.48
	o	7.10 (s)	7.56 (s)	0.46
	p	4.72 (s)	6.22 (s)	1.5
3	a	7.14 (s)	7.69 (s)	0.55
	b	7.76 (s)	8.32 (s)	0.56
	c	7.63 (d, *J* = 8.2 Hz)	7.98 (d, *J* = 8.6 Hz)	0.17
	d	7.77 (d, *J* = 8.1 Hz)	7.97 (d, *J* = 8.4 Hz)	0.20
	e	7.92 (s)	8.18 (s)	0.26
	f	6.99 (s)	7.42 (s)	0.43
	g	6.00 (d, *J* = 7.7 Hz)	7.55 (d, *J* = 7.0 Hz)	1.55
	h	6.53 (t, *J* = 7.8 Hz)	7.80 (t, *J* = 7.6 Hz)	1.27
	i	6.03 (d, *J* = 7.7 Hz)	7.85 (d, *J* = 7.2 Hz)	1.82
	j	7.35 (s)	7.68 (s)	0.33
	k	8.35 (s)	8.37 (s)	0.02
	l	8.01(d, *J* = 8.3 Hz)	8.08 (s)	0.07
	m	7.88(d, *J* = 8.1 Hz)	8.08 (s)	0.20
	n	8.04 (s)	8.35 (s)	0.31
	o	6.98 (s)	7.69 (s)	0.71
	p	6.57 (s)	8.80 (s)	2.23
	q	7.54 (s)	8.47 (s)	0.93

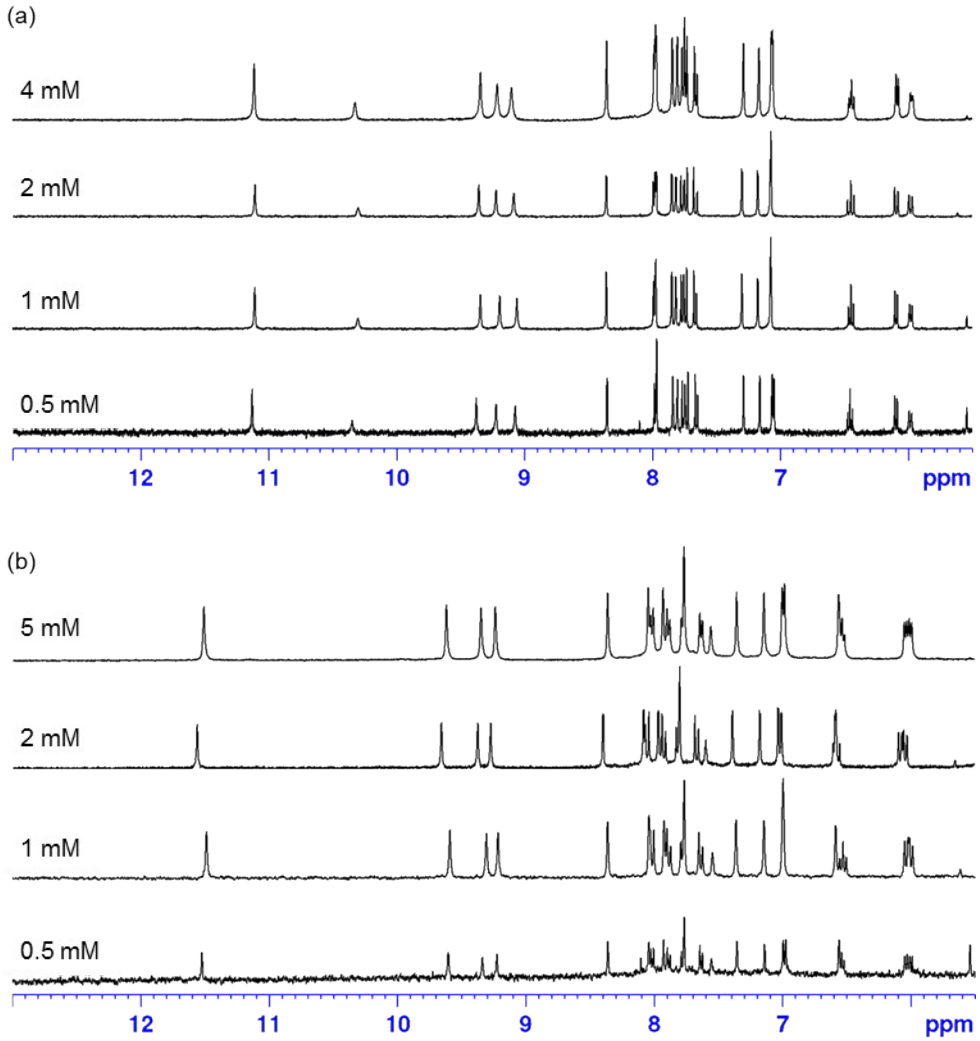

Fig. S3 Concentration-dependent ^{1}H NMR spectra (400 MHz, 25 °C) of (a) **2** and (b) **3** in water-saturated CD_2Cl_2.

2.2 2D-ROESY NMR spectra

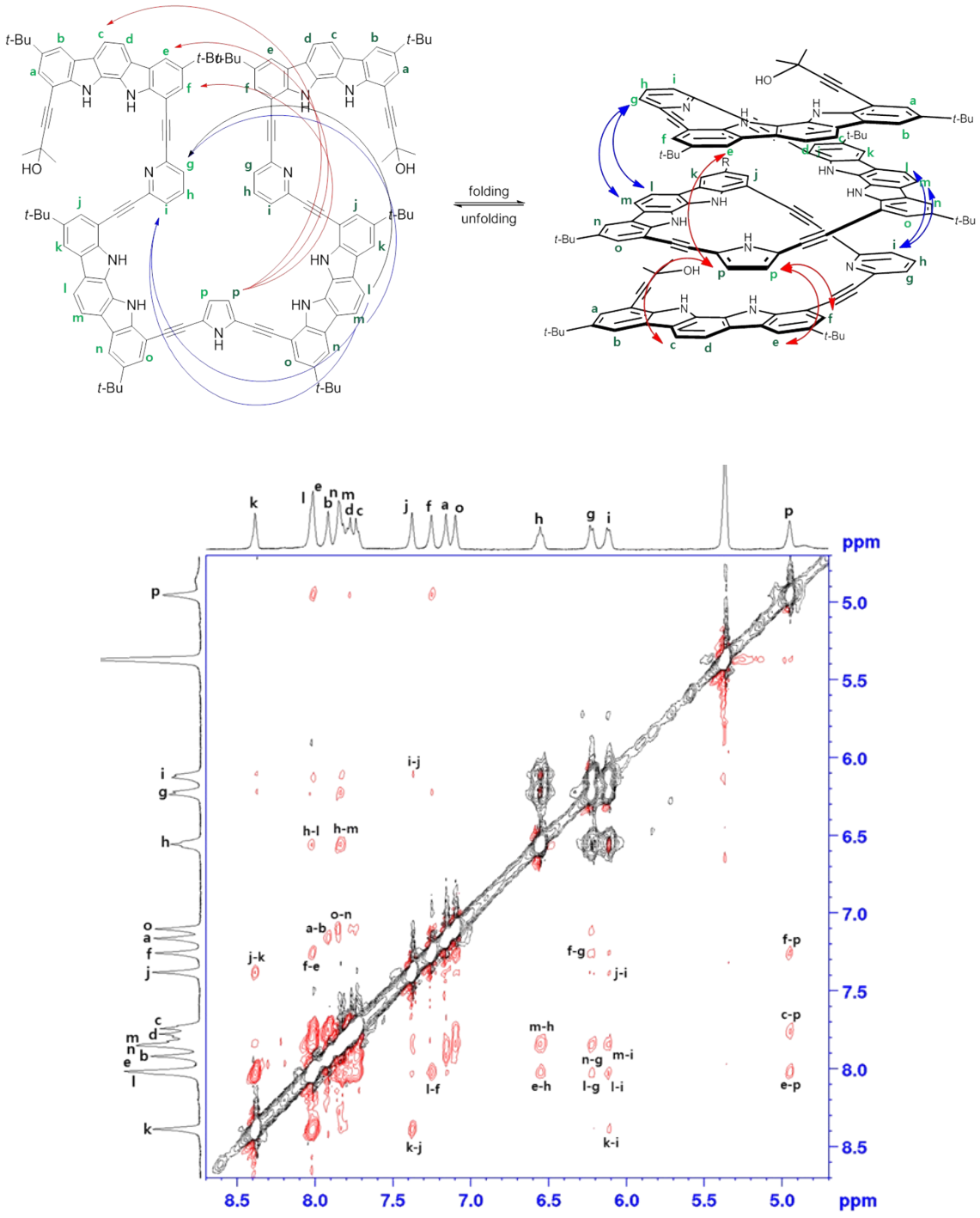

Fig. S4 Partial ROESY spectrum (25 °C, mixing time: 400 ms) of **2** (5.0 mM) in water-saturated CD_2Cl_2.

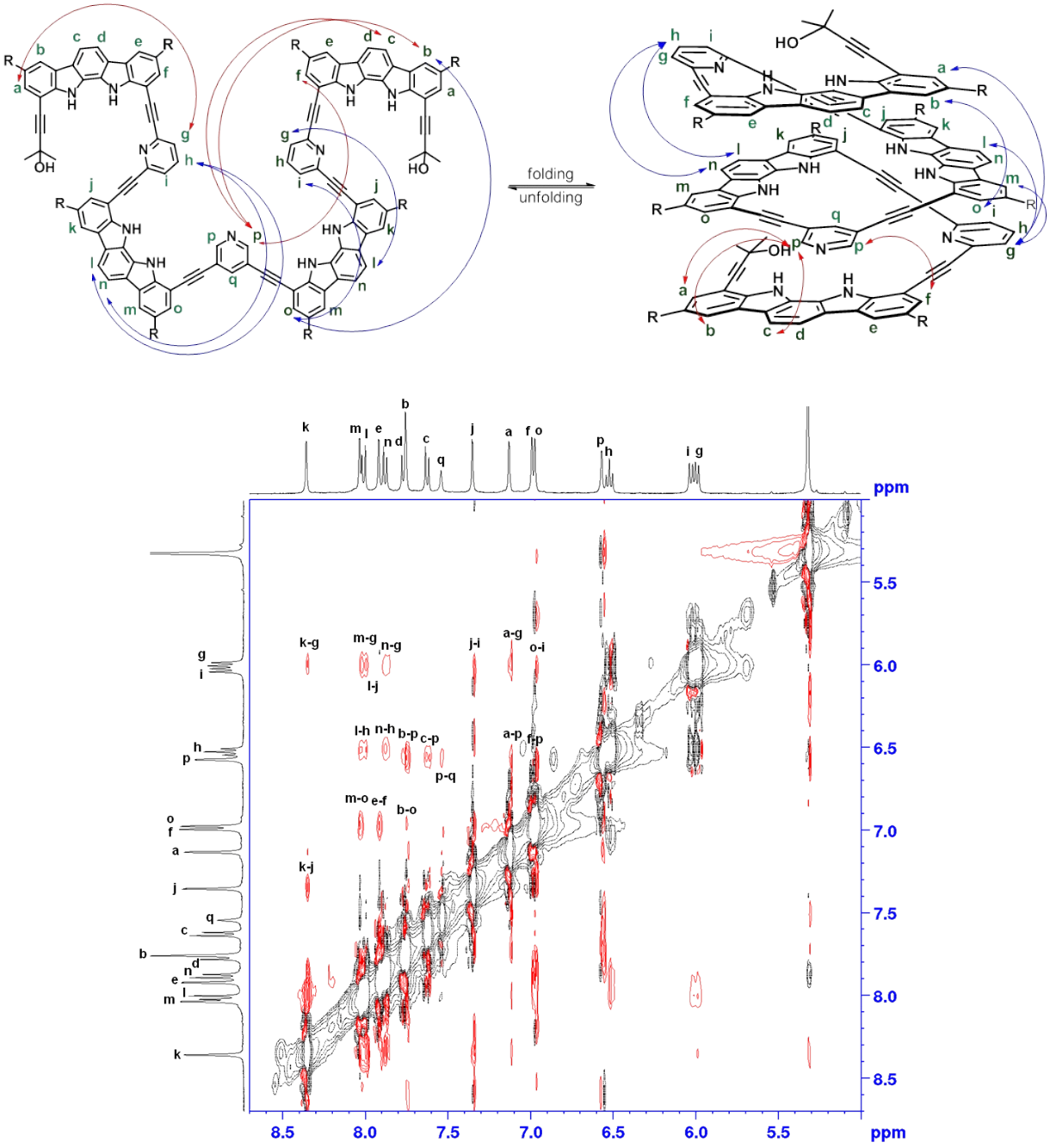

Fig. S5 Partial ROESY spectrum (25 °C, mixing time: 400 ms) of **3** (5.0 mM) in water-saturated CD_2Cl_2.

2.3 Temperature-dependent ^{1}H NMR spectra

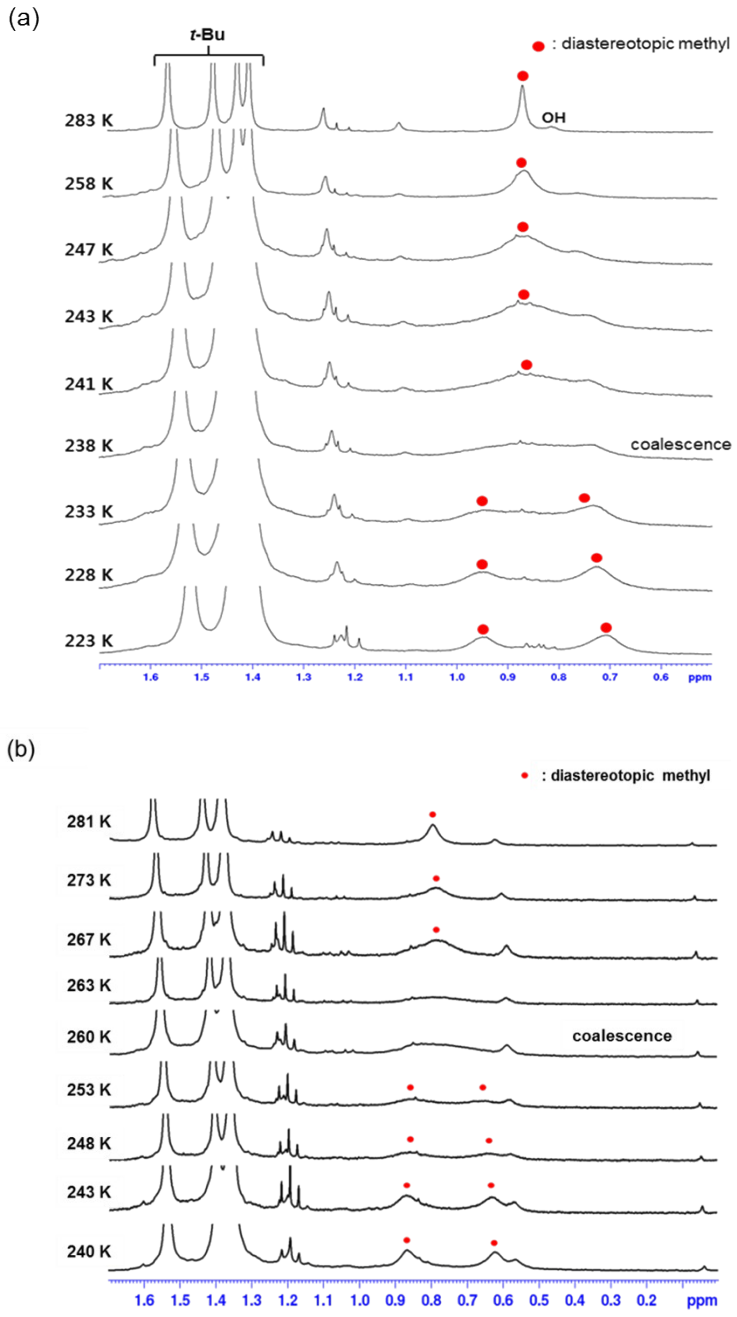

Fig. S6 Temperature-dependent ^{1}H NMR spectra of (a) **2** (2.0 mM) and (b) **3** (2.0 mM) in water-saturated CD_2Cl_2.

The exchange rate constant (k) at the coalescence temperature[S3] was calculated employing the equations (1), (2), (3), (4) and (5) shown below where ν_A and ν_B were the peak

[S3] H. Friebolin, *Basic One- and Two-Dimensional NMR Spectroscopy*, VCH, Weinheim, 1991, 269–273.

frequencies (Hz) of each exchangeable component.

$$\mathrm{A} \underset{k_{-1}}{\overset{k_1}{\rightleftharpoons}} \mathrm{B} \tag{1}$$

$$k = k_1 + k_{-1} \tag{2}$$

$$k = \frac{\pi \Delta v}{\sqrt{2}} \tag{3}$$

$$\Delta v = v_A - v_B \tag{4}$$

$$\Delta G^{\ddagger} = -\mathrm{R}T\ln \frac{kh}{k_B T} \tag{5}$$

(R = 1.9872 cal·K^{-1}·mol^{-1}, k_B = 3.2995 × 10^{-24} cal·K^{-1}, h = 1.5836 × 10^{-34} cal·s)

Table. S2 Activation free energies of **2** and **3** for inter-conversion of *P* and *M* helices in water-saturated CD_2Cl_2.

	method	T (°C)	k_{ex} (s^{-1})	$\Delta G^{\ddagger}$ (kcal·mol^{-1})
2	coalescence	−35	179.5	11.4
3	coalescence	−13	65.9	12.5

3. Binding studies

3.1 ^{1}H NMR titrations

^{1}H NMR titrations: Stock solutions of foldamer **2**, **3** (2.0 mM) and $TBAH_2PO_4$ (10 mM) in water-saturated CD_2Cl_2 were prepared separately at 25 ± 1 °C. A 400 μL portion of the foldamer solution was transferred to a NMR tube, and an initial spectrum was taken to determine the chemical shift of free host. Aliquots of the guest solution were added to the NMR tube and the spectrum was recorded after each addition.

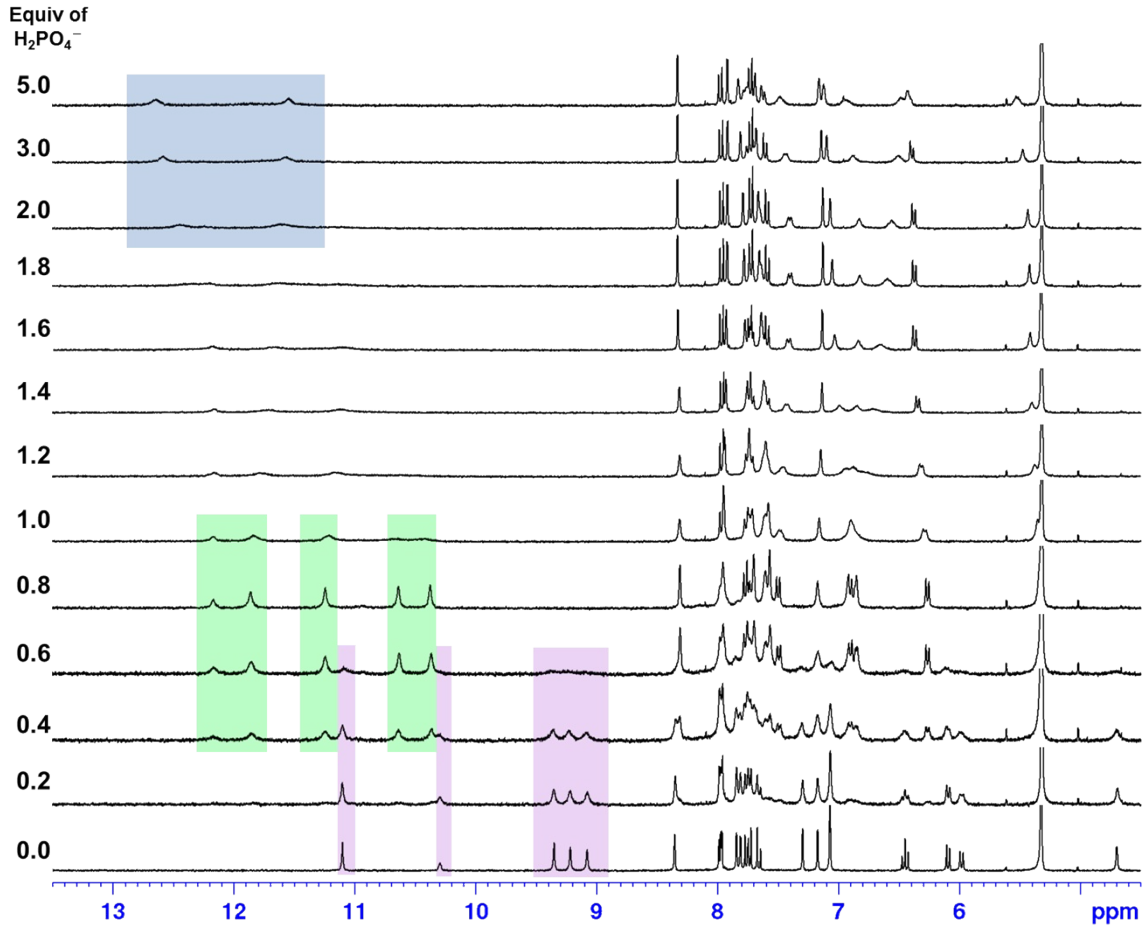

Fig. S7 Partial ^{1}H NMR spectral changes of **2** (2 mM, 25 °C) upon addition of $TBAH_2PO_4$ in water-saturated CD_2Cl_2.

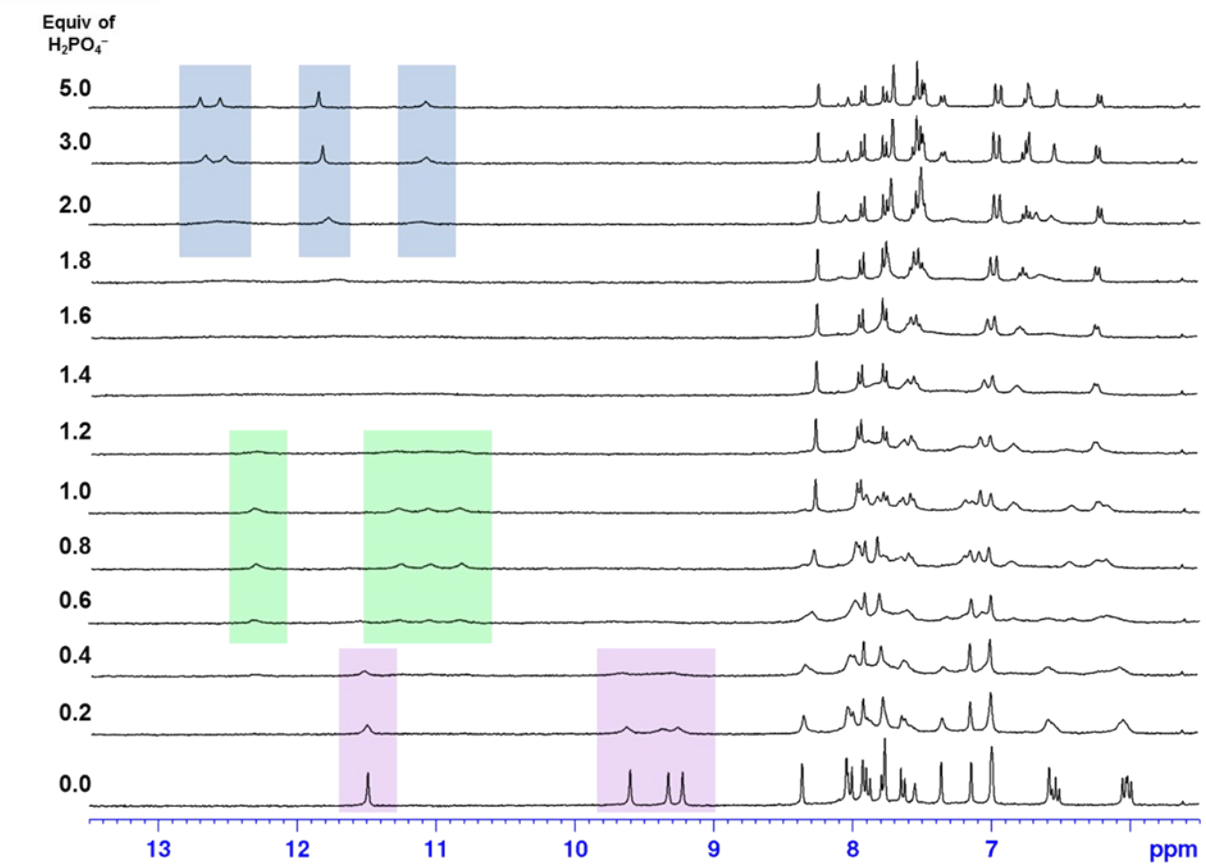

Fig. S8 Partial ^{1}H NMR spectral changes of **3** (2 mM, 25 °C) upon addition of $TBAH_2PO_4$ in water-saturated CD_2Cl_2.

3.2 UV-visible titrations

The UV-visible titrations of foldamers with $TBAH_2PO_4$ were carried out with Agilent 8453 UV–visible spectrophotometer. Solvents of spectroscopic grade solvents were degassed prior to use. For titrations, each stock solution of foldamer **2** or **3** was prepared (1.0×10^{-3} M) in 3% (*v*/*v*) CH_3OH/water-saturated CH_2Cl_2. Separate stock solutions containing different amounts of $TBAH_2PO_4$ were prepared using each foldamer stock solution. A 2 mL portion of each solution was transferred to a cuvette and the spectrum was recorded at 25 °C. The binding constants (log K_1, log K_1K_2 = log β) were determined by WinEQNMR2 program[S4], plotting molar absorptivity at 400 nm and 420 nm for **2**·$TBAH_2PO_4$, and at 360 nm and 400 for **3**·$TBAH_2PO_4$. All the titration curves were fitted to the expression of a 1:2 binding isotherm. Titration experiments were at least duplicated, and errors in the association constants were found to be less than 10% in the association constants.

[S4] M. J. Hynes, *J. Chem. Soc., Dalton Trans.*, 1993, 311.

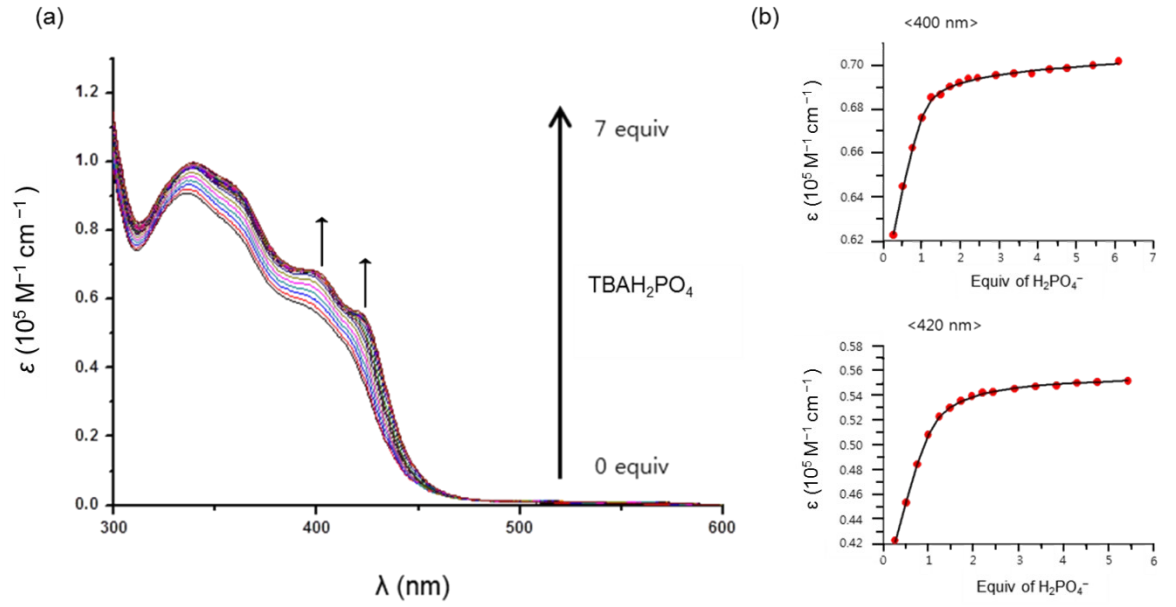

Fig. S9 (a) UV–visible absorption spectral changes of **2** (1.0×10^{-5} M) with increasing the amounts of $TBAH_2PO_4$ in 3% (*v*/*v*) CH_3OH/water-saturated CH_2Cl_2 and (b) titration curves at 400 nm and 420 nm (dot: experimental, line: theoretical).

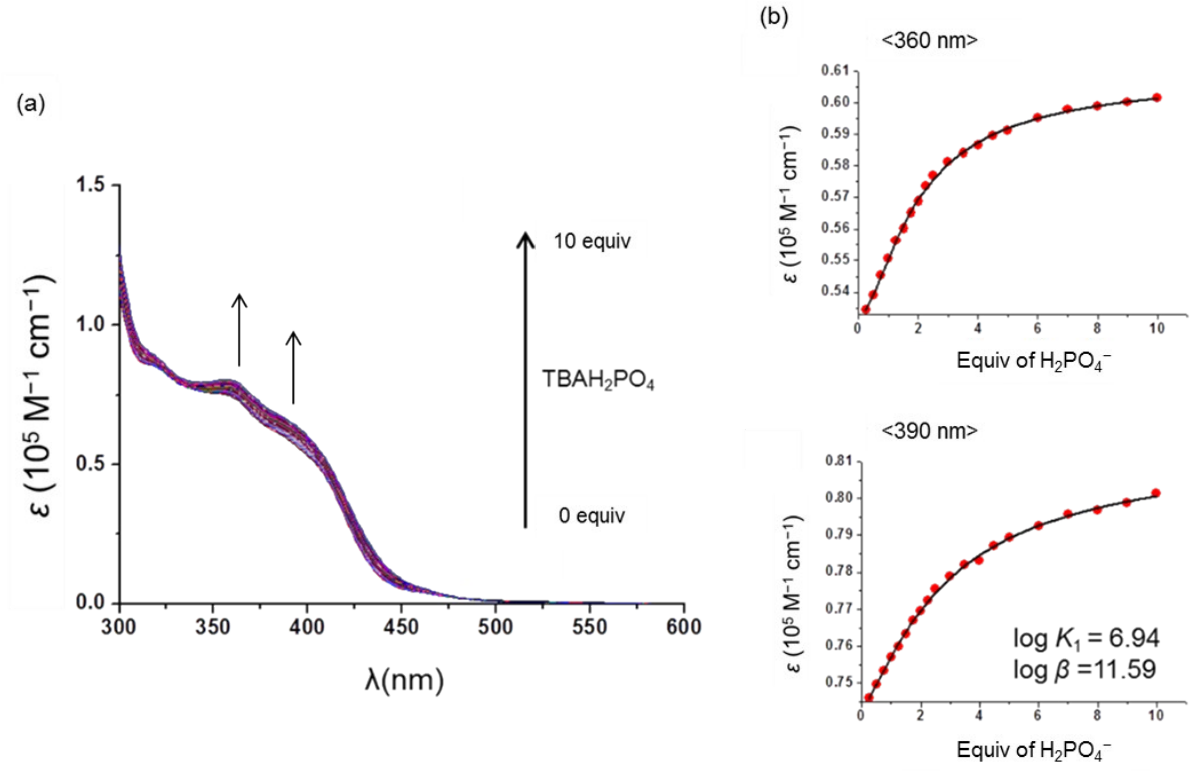

Fig. S10 (a) UV–visible absorption spectral changes **3** (1.0×10^{-5} M) with increasing the amount of $TBAH_2PO_4$ in 3% (*v*/*v*) CH_3OH/water-saturated CH_2Cl_2 and (b) titration curves at 360 nm and 390 nm using WinEQNMR2 program (line: theoretical, dot: experimental).

4. X-ray crystallographic analyses

4.1 Crystal growing

$(H_2PO_4^-)_2 \subset$ **2** : **2** and $TBAH_2PO_4$ (1.5 equiv) was dissolved in tetrahydrofuran and hexane in a test tube, to which solution pentane was slowly vapor-diffused in it at room temperature for a few days to give single crystals suitable for the X-ray diffraction.

$(H_2PO_4^-)_2 \subset$ **3** : **3** and $TBAH_2PO_4$ (2.5 equiv) was dissolved in tetrahydrofuran solution and pentane was slowly vapor-diffused in it at room temperature for a few days to give single crystals suitable for the X-ray diffraction.

4.2 Data collection

Crystals were coated with *Parabar* oil and the diffraction data measured at 100 K with synchrotron radiation (λ = 0.70000 Å) on a Rayonix MX225HS detector at BL2D SMC with a silicon (111) double crystal monochromator at the Pohang Accelerator Laboratory, Korea. The PAL BL2D-SMDC program[S5] was used for data collection (detector distance is 66 mm, omega scan; $\Delta\omega$ = 3º, exposure time is 0.5 sec per frame) and HKL3000sm (Ver. 716.7)[S6] was used for cell refinement, reduction and absorption correction.

4.3 Structure solution and refinement

The crystal structures were solved by the direct method with SHELX-XT[S7] and refined by full-matrix least-squares calculations with the SHELX-XL[S8] in the Olex2[S9] program package. The structure solutions of crystals were obtained by the direct methods provided most non-hydrogen atoms from the E-map. The remaining non-hydrogen atoms were located in an alternating series of least-squares cycles and difference Fourier maps. All non-hydrogen atoms were refined with anisotropic displacement coefficients. All hydrogen atoms were included in the structure factor calculation at idealised positions and were allowed to ride on the neighboring atoms with relative isotropic displacement coefficients.

[S5] J. W. Shin, K. Eom and D. Moon, PAL BL2D-SMDC Program, *J. Synchrotron Radiat.*, 2016, **23**, 369–373.

[S6] Z. Otwinowski and W. Minor, in *Methods in Enzymology*, ed. C. W. Carter Jr. and R. M. Sweet, Academic Press, 1997, **276**, 307.

[S7] G. Sheldrick, *Acta Crystallogr., Sect. A: Fundam. Crystallogr.*, 2015, **71**, 3–8.

[S8] G. Sheldrick, *Acta Crystallogr., Sect. C: Cryst. Struct. Commun.*, 2015, **71**, 3–8.

[S9] O. V. Dolomanov, L. J. Bourhis, R. J. Gildea, J. A. K. Howard and H. Puschmann, *J. Appl. Crystallogr.*, 2009, **42**, 339–341.

For $(H_2PO_4^-)_2 \subset$ **2**, two *t*-butyl groups bonded to an indolocarbazole were observed as disordered and modeled using SADI and ISOR restraints. The final least-squares refinement of 972 parameters against 22866 data resulted in residuals R (based on F^2 for $I \geq 2\sigma$) and wR (based on F^2 for all data) of 0.0712 and 0.1857, respectively. The final difference Fourier map was featureless.

For $(H_2PO_4^-)_2 \subset$ **3**, two *t*-butyl groups bonded to an indolocarbazole were observed as disordered and modeled using SADI and ISOR restraints. The final least-squares refinement of 975 parameters against 24407 data resulted in residuals R (based on F^2 for $I \geq 2\sigma$) and wR (based on F^2 for all data) of 0.0904 and 0.2822, respectively. The final difference Fourier map was featureless.

4.4 Summary

$(H_2PO_4^-)_2 \subset$ **2**: Crystal Data for $C_{172}H_{203}N_{13}O_{10}P_2$ (M =2674.40 g/mol): monoclinic, space group C2/c (no. 15), a = 21.469(4) Å, b = 29.096(6) Å, c = 28.543(6) Å, β = 95.17(3)°, V = 17757(6) Å^3, Z = 4, T = 100 K, μ(synchrotron) = 0.077 mm^{-1}, *Dcalc* = 1.000 g/cm^3, 45276 reflections measured (2.634° ≤ 2Θ ≤ 57°), 22866 unique (R_{int} = 0.0958, R_{sigma} = 0.1684) which were used in all calculations. The final R_1 was 0.0712 (I > 2σ(I)) and wR_2 was 0.1857 (all data).

$(H_2PO_4^-)_2 \subset$ **3** : Crystal Data for $C_{173}H_{203}N_{13}O_{10}P_2$ (M =2686.41 g/mol): monoclinic, space group C2/c (no. 15), a = 21.505(4) Å, b = 29.114(6) Å, c = 28.751(6) Å, β = 94.83(3)°, V = 17937(6) Å^3, Z = 4, T = 100 K, μ(synchrotron) = 0.076 mm^{-1}, *Dcalc* = 0.995 g/cm^3, 94417 reflections measured (2.794° ≤ 2Θ ≤ 57.998°), 24407 unique (R_{int} = 0.0737, R_{sigma} = 0.0645) which were used in all calculations. The final R_1 was 0.0904 (I > 2σ(I)) and wR_2 was 0.2822 (all data).

Table. S3 Crystal data and structure refinement for $(H_2PO_4^-)_2 \subset \mathbf{2}$

Identification code	$(H_2PO_4^-)_2 \subset \mathbf{2}$
Empirical formula	$C_{172}H_{203}N_{13}O_{10}P_2$
Formula weight	2674.40
Temperature/K	100
Crystal system	monoclinic
Space group	C2/c
a/Å	21.469(4)
b/Å	29.096(6)
c/Å	28.543(6)
α/°	90
β/°	95.17(3)
γ/°	90
Volume/Å^3	17757(6)
Z	4
Dcalc g/cm^3	1.000
μ/mm^{-1}	0.077
F(000)	5744.0
Crystal size/mm^3	0.203 × 0.026 × 0.026
Radiation	synchrotron (λ = 0.70000)
2Θ range for data collection/°	2.634 to 57
Index ranges	$-29 \le h \le 29$, $-39 \le k \le 39$, $-37 \le l \le 37$
Reflections collected	45276
Independent reflections	22866 [R_{int} = 0.0958, R_{sigma} = 0.1684]
Data/restraints/parameters	22866/42/972
Goodness-of-fit on F^2	0.828
Final R indexes [$I > 2\sigma(I)$]	R_1 = 0.0712, wR_2 = 0.1519
Final R indexes [all data]	R_1 = 0.1761, wR_2 = 0.1857
Largest diff. peak/hole / e.Å^{-3}	0.43/-0.38

Table. S4 Crystal data and structure refinement for $(H_2PO_4^-)_2 \subset \mathbf{3}$

Identification code	$(H_2PO_4^-)_2 \subset \mathbf{3}$
Empirical formula	$C_{173}H_{203}N_{13}O_{10}P_2$
Formula weight	2686.41
Temperature/K	100
Crystal system	monoclinic
Space group	C2/c
a/Å	21.505(4)
b/Å	29.114(6)
c/Å	28.751(6)
α/°	90
β/°	94.83(3)
γ/°	90
Volume/Å^3	17937(6)
Z	4
Dcalc g/cm^3	0.995
μ/mm^{-1}	0.076
F(000)	5768.0
Crystal size/mm^3	0.296 × 0.078 × 0.07
Radiation	synchrotron (λ = 0.70000)
2Θ range for data collection/°	2.794 to 57.998
Index ranges	$-29 \le h \le 29$, $-40 \le k \le 40$, $-38 \le l \le 38$
Reflections collected	94417
Independent reflections	24407 [R_{int} = 0.0737, R_{sigma} = 0.0645]
Data/restraints/parameters	24407/73/975
Goodness-of-fit on F^2	1.017
Final R indexes [$I > 2\sigma(I)$]	R_1 = 0.0904, wR_2 = 0.2576
Final R indexes [all data]	R_1 = 0.1314, wR_2 = 0.2822
Largest diff. peak/hole / e.Å^{-3}	1.04/-0.65

Table. S5 Hydrogen bonds and their distances (Å) of the (a) upper half and (b) lower half in the X-ray crystal structure of $(H_2PO_4^-)_2 \subset$ **2**.

(a)

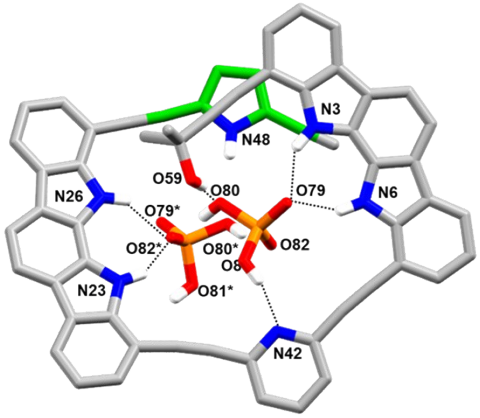

Donor···Acceptor	Distance
N3···O79	2.812
N6···O79	2.701
O81···N42	2.708
N23···O82*	2.996
N26···O82*	2.892
O59···O80	2.836

(b)

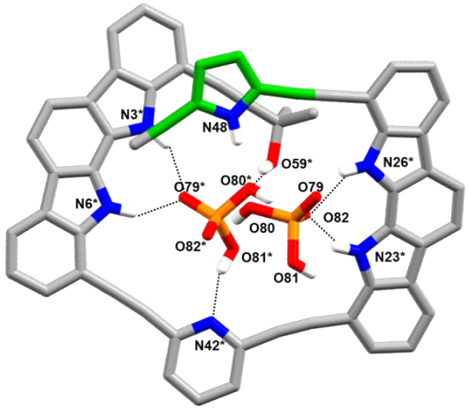

Donor···Acceptor	Distance
N3*···O79*	2.812
N6*···O79*	2.701
O81*···N42*	2.708
N23*···O82	2.996
N26*···O82	2.892
O59*···O80*	2.836

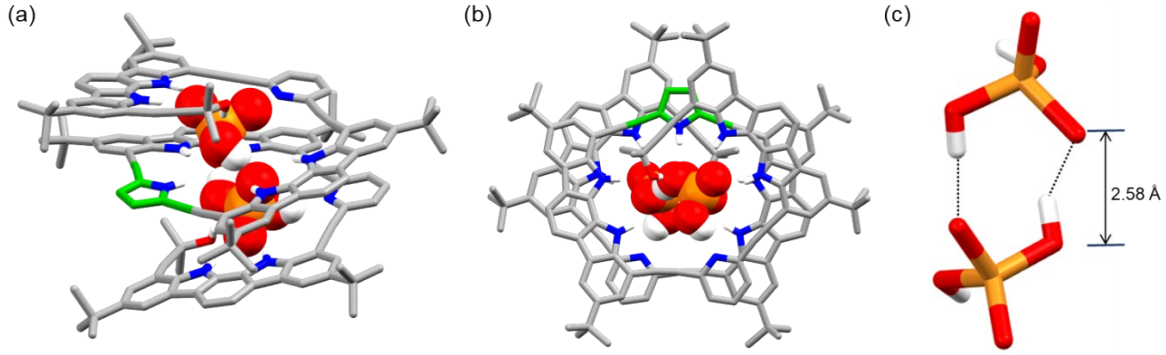

Fig. S11 X-ray crystal structures of $(H_2PO_4^-)_2 \subset$ **2** of (a) top view and (b) side view. (c) Dimeric dihydrogenphosphate ions via cyclic hydrogen bonds. Hydrogen atoms attached to carbon atoms are omitted for clarity.

Table. S6 Hydrogen bonds and their distances (Å) of the (a) upper half and (b) lower half in the X-ray crystal structure of $(H_2PO_4^-)_2 \subset \mathbf{3}$.

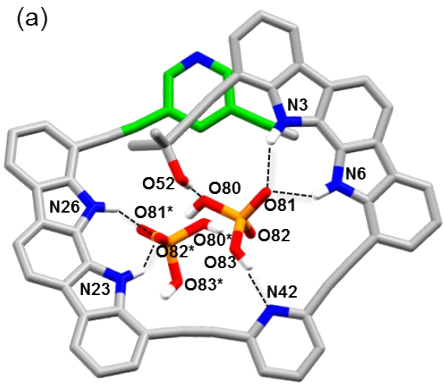

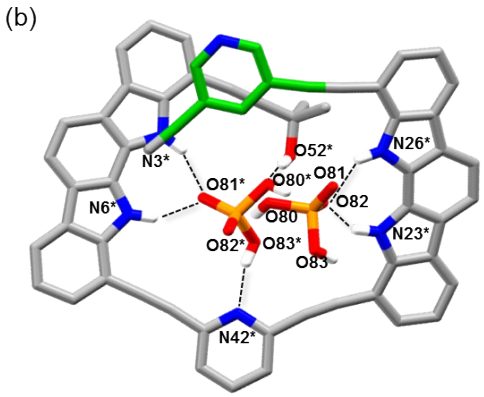

Donor···Acceptor	Distance (Å)
N3···O81	2.778
N6···O81	2.708
N42···O83	2.705
N23*···O82	2.961
N26*···O82	2.893
O52···O80	2.813

Donor···Acceptor	Distance (Å)
N3*···O81*	2.778
N6*···O81*	2.708
N42*···O83*	2.705
N23···O82*	2.961
N26···O82*	2.893
O52*···O80*	2.813

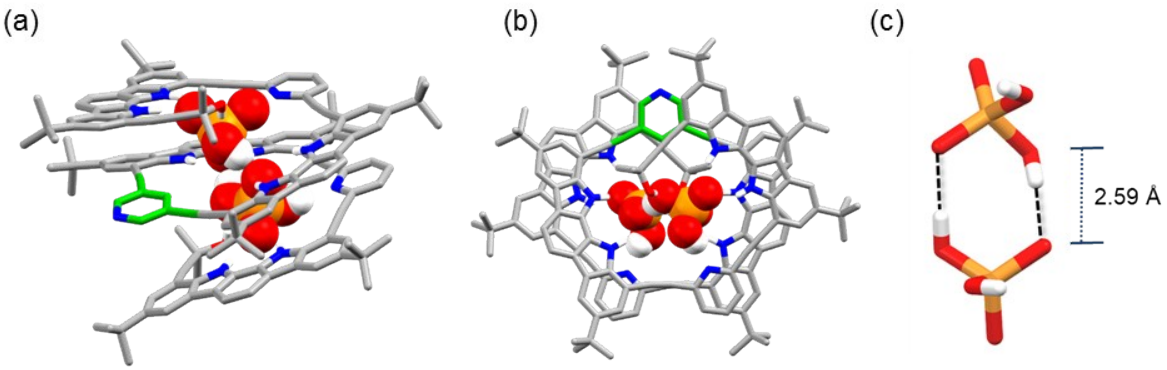

Fig. S12 Crystal structure of $(H_2PO_4^-)_2 \subset \mathbf{3}$ of (a) side view and (b) Top view (c) Dimeric dihydrogenphosphate ions via cyclic hydrogen bonds. Hydrogen atoms attached to carbon atoms are omitted for clarity.

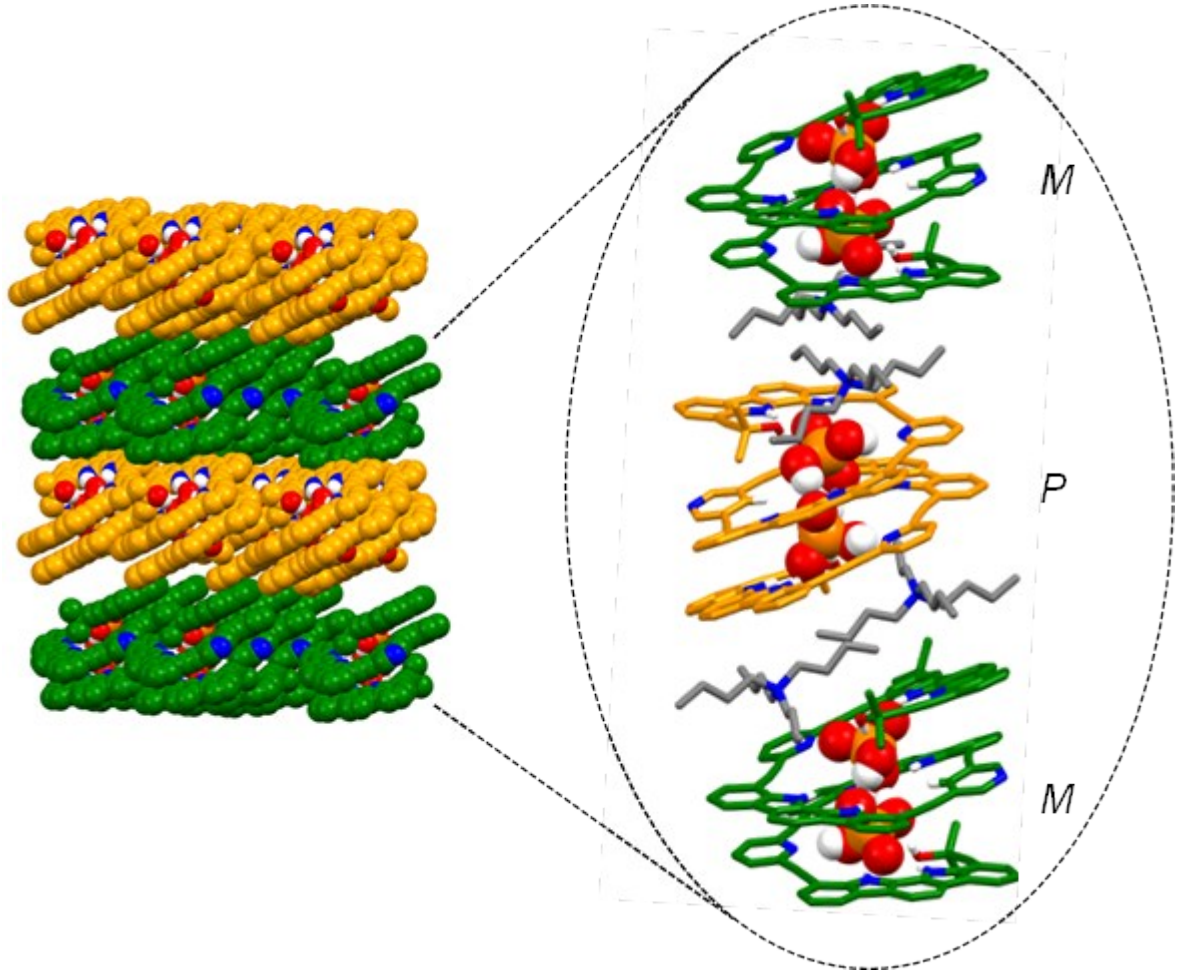

Fig. S13 Packing views of the crystal structure of $(H_2PO_4^-)_2 \subset$ **3**. Yellow and green helices are represented *P* and *M* helices. Tetrabutylammonium cations are shown in grey and *t*-butyl groups are omitted for clarity.